Brachypodium distachyon line Bd3-1 resistance is elicited by the barley stripe mosaic virus triple gene block 1 movement protein

Mi Yeon Lee,[1]† Lijie Yan,[2]† Florien A. Gorter,[1,3] Brian Y. T. Kim,[1] Yu Cui,[1,2] Yue Hu,[2] Cheng Yuan,[2] Jessica Grindheim,[1] Uma Ganesan,[1] Zhiyong Liu,[2] Chenggui Han,[2] Jialin Yu,[2] Dawei Li[2] and Andrew O. Jackson[1]

Correspondence
Andrew O. Jackson
andyoj@berkeley.edu
Dawei Li
Dawei.Li@cau.edu.cn

[1]Department of Plant and Microbial Biology, University of California–Berkeley, Berkeley, CA 94720, USA

[2]State Key Laboratory of Agro-Biotechnology, China Agricultural University, Beijing 100193, PR China

[3]Laboratory of Genetics, Department of Plant Sciences, Wageningen University, 6700 AH Wageningen, The Netherlands

Barley stripe mosaic virus North Dakota 18 (ND18), Beijing (BJ), Xinjiang (XJ), Type (TY) and CV21 strains are unable to infect the *Brachypodium distachyon* Bd3-1 inbred line, which harbours a resistance gene designated *Bsr1*, but the Norwich (NW) strain is virulent on Bd3-1. Analysis of ND18 and NW genomic RNA reassortants and RNAβ mutants demonstrates that two amino acids within the helicase motif of the triple gene block 1 (TGB1) movement protein have major effects on their Bd3-1 phenotypes. Resistance to ND18 correlates with an arginine residue at TGB1 position 390 (R^{390}) and a threonine at position 392 (T^{392}), whereas the virulent NW strain contains lysines (K) at both positions. ND18 TGB1 R390K ($_{ND}TGB1_{R390K}$) and $_{ND}TGB1_{T392K}$ single substitutions, and an $_{ND}TGB1_{R390K,T392K}$ double mutation resulted in systemic infections of Bd3-1. Reciprocal $_{ND}TGB1$ substitutions into $_{NW}TGB1$ ($_{NW}TGB1_{K390R}$ and $_{NW}TGB1_{K392T}$) failed to affect virulence, implying that K^{390} and K^{392} compensate for each other. In contrast, an $_{NW}TGB1_{K390R,K392T}$ double mutant exhibited limited vascular movement in Bd3-1, but developed prominent necrotic streaks that spread from secondary leaf veins. This phenotype, combined with the appearance of necrotic spots in certain ND18 mutants, and necrosis and rapid wilting of Bd3-1 plants after BJ strain ($_{BJ}TGB1_{K390,T392}$) inoculations, show that Bd3-1 *Bsr1* resistance is elicited by the TGB1 protein and suggest that it involves a hypersensitive response.

INTRODUCTION

Barley stripe mosaic virus (BSMV) exhibits enormous phenotypic variation that depends both on the virus strain and on the infected host variety (Petty *et al.*, 1994). BSMV was one of the first viruses for which extensive strain mutants were collected and, by 1965, more than 25 strains had been described that elicited different symptom phenotypes on several cereals and some dicots (McKinney & Greeley, 1965). Over the past half century, BSMV has been shown to occur naturally in field infections of several cereals, in addition to barley, and has been transmitted experimentally to many wild grasses and several dicot species (Jackson &

Lane, 1981), as well as some tropical monocots (Renner *et al.*, 2009). Disease phenotypes in these hosts range from mild stunting and mosaic symptoms to severe chlorosis, necrotic local lesions and systemic lethal syndromes, as well as developmental anomalies. Reverse genetic analyses of the BSMV Type and North Dakota 18 (ND18) strains has revealed that most virus-induced phenotypes examined map to variations in the γb pathogenesis gene and the γa replicase subunit (Donald & Jackson, 1994; Santoso & Edwards, 2003; Jackson *et al.*, 1991a, b; Weiland & Edwards, 1996).

In contrast, very little is known about host gene effects on BSMV disease phenotypes (Edwards *et al.*, 2006) because modern genomics applications have not been developed for cereals until relatively recently. However, we have found that several BSMV strains cause different infection phenotypes on purple false brome [*Brachypodium distachyon* (L.) P.

---

†These authors contributed equally to this work.

Supplementary results, methods and tables are available with the online version of this paper.

Beavu], a wild grass that has been developed as a model host for cereal genomics (Brkljacic *et al.*, 2011; Garvin *et al.*, 2008; Opanowicz *et al.*, 2008; Vogel & Bragg, 2009). Among several *B. distachyon* lines tested, the BSMV ND18 strain is able to infect line Bd21, and infected plants exhibit mild to intense mosaic symptoms, stunting and failure to set seeds, and contain large amounts of virus (Cui *et al.*, 2012). In contrast, the Bd3-1 line is resistant to ND18 and harbours a temperature-sensitive resistance (R) gene designated barley stripe resistance 1 (*Bsr1*) (Cui *et al.*, 2012). We have used Bd21 × Bd3-1 F$_2$ crosses and an F$_6$ recombinant inbred line (RIL) population resulting from a Bd3-1 × Bd21 cross to investigate the genetics of *Bsr1* and have shown that *Bsr1* is a single dominant R gene (Cui *et al.*, 2012) that differs from BSMV R genes in barley and oats that are generally recessive (Edwards *et al.*, 2006). Hence, the *Bsr1* R gene represents a departure from the R genes that have originated during cereal cultivation. We also have generated an F$_6$ RIL genetic linkage map to locate *Bsr1* within a 23 kb region at the top of chromosome (Chr) 3 and our initial analyses indicated that the mapped region of Bd21 contains five ORFs, including a putative R gene (Cui *et al.*, 2012). However, more recently released sequence information has shown that the Bd3-1 strain has undergone a deletion event, and retains the putative R gene, but not the other four ORFs (http://genomesonline.org/cgi-bin/GOLD/bin/GOLDCards.cgi?gold stamp=Gr00035).

Moreover, our genomics analyses reveal that both Bd21 (Vogel *et al.*, 2010) and Bd3-1 harbour related R alleles within the mapped region of Chr 3, but that the candidate R alleles vary in their sizes and in their predicted functions. The putative Bd3-1 R gene specifies a protein with N-terminal coiled-coil (CC) and NBS (also called NB-ARC) domains (van Ooijen *et al.*, 2008) and a C-terminal 'leucine-rich repeat' (LRR) domain that is structurally similar to several dominant R genes that specify resistance to viral, bacterial and fungal hosts (Gururani *et al.*, 2012; Kang *et al.*, 2005; Maule *et al.*, 2007; Moffett, 2009; Whitham *et al.*, 1994). In contrast, the Bd21 R allele lacks the LRR domain that is thought to be involved in protein–protein interactions and probably represents a non-functional allele. Because the Bd3-1 R gene appears to have a functional motif, our analyses suggest that the CC-NBS-LRR allele corresponds to *Bsr1*.

Our recent results have shown that the BSMV Norwich (NW) strain is able to circumvent Bd3-1 resistance, and that NW infections of Bd3-1 and Bd21 result in nearly identical phenotypes. Here, we report genome-reassortant experiments demonstrating that the major NW virulence determinant resides within RNAβ, which encodes the coat protein (CP) and three overlapping triple gene block (TGB) movement proteins designated TGB1, TGB2 and TGB3 (Jackson *et al.*, 2009; Verchot-Lubicz *et al.*, 2010). We have constructed ND18 RNAβ ($_{ND}$RNAβ) and $_{NW}$RNAβ chimeras and have shown that a sequence block containing two critical amino acid residues within the helicase motif of Norwich TGB1 ($_{NW}$TGB1) affects the ability to infect Bd3-1.

Among the infection phenotypes observed, those of some TGB1 mutants containing site-specific mutations of the two TGB1 amino acid residues (positions 390 and 392) elicit a striking necrosis on leaves emerging 5–7 days post-inoculation (p.i.), but these leaves appear to accumulate very low levels of virus. We provide a model whereby the $_{ND}$TGB1 protein interacts with the Bd3-1 *Bsr1* protein to elicit a hypersensitive response (HR) that constrains ND18 infections, whereas the $_{NW}$TGB1 and *Bsr1* proteins fail to interact and elicit resistance, hence permitting NW to establish systemic infections on Bd3-1.

RESULTS

BSMV ND18 and NW phenotypes differ in the *B. distachyon* line Bd3-1

Previously constructed biologically active ND18 cDNA clones have been reported (Petty *et al.*, 1989), and NW RNA cloning and sequencing are described in the supplementary Methods (available in JGV Online). Comparisons of the deduced ND18 RNA ($_{ND}$RNA) and Norwich RNA ($_{NW}$RNA) sequences reveal several minor differences in their coding regions, and these are shown in the codon maps of RNAs α, β and γ (illustrated in Fig. S1). The infectivity of *in vitro* transcripts synthesized from linearized NW (pT7α_{NW}, pT7β_{NW} and pT7γ_{NW}) and ND18 (pT7α_{ND}, pT7β_{ND} and pT7γ_{ND}) plasmids were tested by mechanically inoculating barley, and the *B. distachyon* lines Bd21-3, Bd21 and Bd3-1 (Fig. 1). All inoculated barley varieties developed typical systemic mosaic symptoms by about 5–7 days p.i. (Fig. 1a), and the NW and ND18 strains were also virulent on lines Bd21-3 and Bd21, which normally developed systemic mosaic symptoms on emerging leaves by 7 days p.i. accompanied by high levels of viral RNA in leaf extracts (Fig. 1b, c). In contrast, Bd3-1 plants exhibited a differential phenotype when infected with NW and ND18 (Fig. 1d). The NW strain was virulent on Bd3-1; however, as shown previously, the ND18 strain was unable to infect Bd3-1, which contains the *Bsr1* gene (Cui *et al.*, 2012), and inoculated plants failed to exhibit signs of infection and detectable amounts of BSMV RNAs did not accumulate (Fig. 1d).

TGB1 determinants affect Bd3-1 resistance

For more detailed comparisons, ND18 and NW α, β and γ genomic RNA (gRNA) reassortants, and a series of RNAβ chimeras and site-specific mutants were used to delineate the region responsible for NW virulence on *B. distachyon* line Bd3-1. ND18 and NW α, β and γ *in vitro* transcripts were mixed in all possible combinations and inoculated into barley (data not shown), and the *B. distachyon* Bd3-1 and Bd21 lines (Fig. 2). Again, Bd3-1 plants inoculated with ND18 did not develop symptoms, but with wild-type (wt)NW or transcript reassortants containing $_{NW}$RNAβ, Bd3-1 exhibited fully susceptible phenotypes (Fig. 2a). In
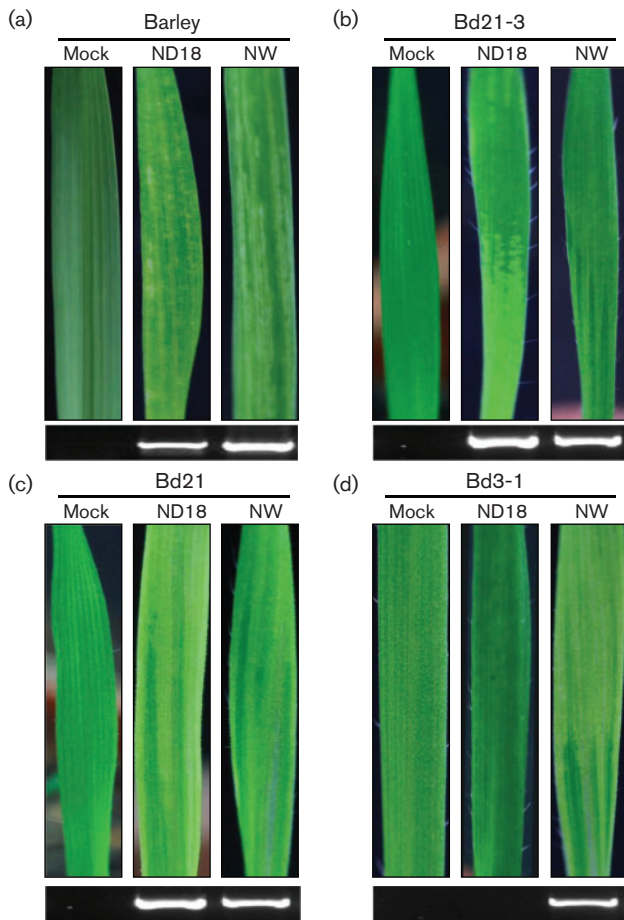
Fig. 1. Symptoms and RT-PCR detection of BSMV ND18 and NW strain infections on barley and the *B. distachyon* lines Bd21-3, Bd21 and Bd3-1. (a) Appearance of emerging uninoculated leaves of barley plants at 7 days p.i. (top), and RT-PCR detection (bottom) of BSMV RNAγ with specific primers BS-10 and BS-32 (see Table S1). Note the upper uninoculated leaves of the BSMV-inoculated barley have typical chlorotic stripes and mosaic symptoms. (b, c) Typical systemic BSMV ND18 and NW symptoms (top) and RT-PCR (bottom) at 14 days p.i. on emerging leaves of mock-inoculated or BSMV-inoculated *B. distachyon* line Bd21-3 (b) or line Bd21 (c). (d) Differential virulence of BSMV strains on *B. distachyon* line Bd3-1. The ND18 strain is unable to infect Bd3-1 and elicits resistance in which visible symptoms or accumulation of BSMV RNA are not evident on leaves emerging after inoculation, whereas NW is virulent and inoculated plants develop systemic infections on the emerging leaves, which accumulate high levels of BSMV RNA, similar to Bd21 infections with the ND18 and NW strains.
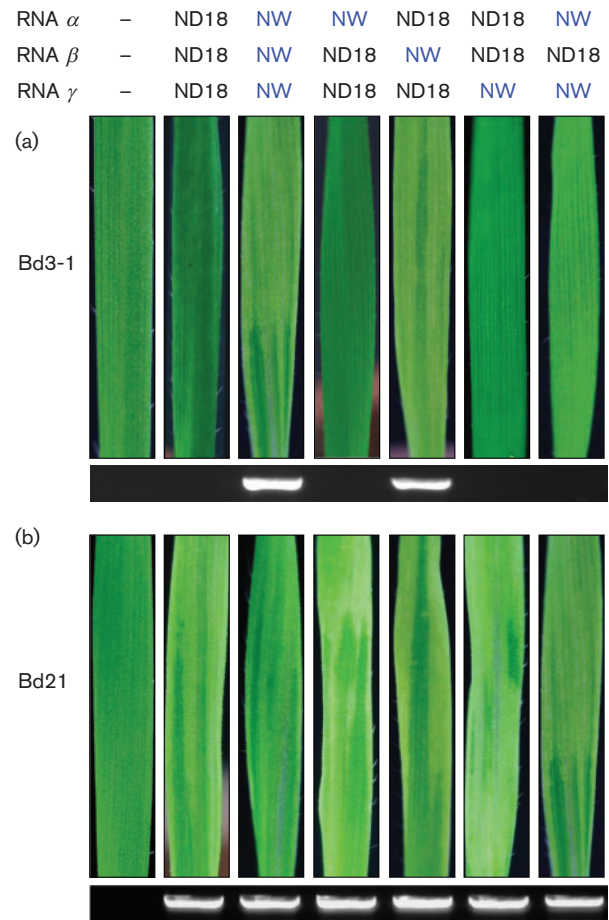
Fig. 2. Identification of ND18 and NW BSMV gRNA requirements for infection of *B. distachyon* Bd3-1 and Bd21 lines. ND18 and NW strain α, β and γ wtRNAs were transcribed *in vitro* and inoculated in all possible combinations into Bd3-1 (a) and Bd21 (b) seedlings. Top: phenotype on emerging leaves of inoculated plants. Bottom: RT-PCR detection of BSMV RNA in leaves. Note: all ND18 RNA (ND RNA) and NW (NW RNA) combinations were able to infect barley (data not shown) and Bd21, but only combinations containing NW RNAβ elicited a systemic mosaic infection phenotype on Bd3-1 leaves. Leaves showing systemic symptoms also accumulated high levels of virus as assessed by RT-PCR to detect BSMV RNA or ELISA to evaluate CP accumulation (data not shown), whereas uninfected plants failed to exhibit detectable amounts of BSMV RNA or CP.

these cases, the uninoculated emerging leaves developed strong mosaic symptoms and accumulated high levels of BSMV RNA (Fig. 2a). Occasionally, leaves of Bd3-1 plants inoculated with $_{NW}$RNAγ reassortants developed a mild mottling phenotype with small amounts of necrosis, but this phenotype was not reproducible, and the leaves did not

contain CP or viral RNA (data not shown). Therefore, we believe that these inconsistencies result from unidentified environmental stresses and/or unspecific biotrophic interactions (Cui *et al.*, 2012). In summary, the results demonstrate that $_{ND}$RNAβ encodes the primary determinants that elicit Bd3-1 resistance, and that $_{ND}$RNAα and γ have negligible contributions to the resistance phenotype.

To further delineate the RNAβ region responsible for Bd3-1 resistance to ND18, chimeric pT7β clones were constructed by restriction fragment substitutions between the pT7β$_{ND}$

and pT7β_{NW} plasmids (see supplementary Methods). A unique *Pst*I restriction site common to both plasmids is located approximately halfway along each cDNA insert near the middle of the TGB1 ORF (Fig. 3a). This site was used to construct complementary chimeric clones ($\beta_{ND}NW_{Ps-3'}$ and $\beta_{NW}ND_{Ps-3'}$) containing about equal amounts of pT7β_{ND} and pT7β_{NW}. The $\beta_{ND}NW_{Ps-3'}$ plasmid contains 5′ ND18 and 3′ NW sequences, whereas $\beta_{NW}ND_{Ps-3'}$ consists of 5′ NW and 3′ ND18 sequences (Fig. 3a). By 7–14 days p.i., inocula containing the chimeric RNAβ derivatives and $_{ND}$RNAα and $_{ND}$RNAγ transcribed from pT7α_{ND} and pT7γ_{ND} elicited systemic infections on barley (data not shown) and Bd21, where positive RT-PCR and ELISA results were obtained (Fig. 3b). In contrast, the respective susceptible and resistant infection phenotypes of the $\beta_{ND}NW_{Ps-3'}$ and the $\beta_{NW}ND_{Ps-3'}$ chimeras clearly revealed that the 3′ half of $_{ND}$RNAβ contains a determinant responsible for eliciting Bd3-1 resistance (Fig. 3).

For more refined mapping of RNAβ determinants responsible for the disease phenotype, the *Pst*I site and a common *Eco*RI site located about 65 % of the distance from the 5′ end of the RNAβ sequence in the pβ plasmids were used to generate chimeras designated $\beta_{ND}NW_{Ec-3'}$, $\beta_{ND}NW_{Ps-Ec}$ and $\beta_{NW}ND_{Ps-Ec}$ (Fig. 3a). Inocula containing mixtures of $_{ND}$RNAα and $_{ND}$RNAγ and each of the chimeric RNAβ derivatives again were fully virulent on barley (data not shown) and Bd21, but their virulence on Bd3-1 varied (Fig. 3b). The $\beta_{ND}NW_{Ps-Ec}$ RNA combination was able to infect Bd3-1 systemically and produced mosaic symptoms similar to those of the NW strain on Bd3-1 (Fig. 3b, lane $\beta_{ND}NW_{Ps-Ec}$). In contrast, $\beta_{NW}ND_{Ps-Ec}$ chimeric RNAs failed to elicit Bd3-1 leaf symptoms or accumulate detectable levels of viral RNA (Fig. 3b, lane $\beta_{NW}ND_{Ps-Ec}$), or CP in emerging leaves (data not shown). These results demonstrate that the $_{ND}$RNAβ *Pst*I–*Eco*RI fragment is involved in TGB1 elicitation of Bd3-1 resistance. However, inoculation of $\beta_{ND}NW_{Ec-3'}$ combinations to Bd3-1 produced a phenotype in which emerging Bd3-1 leaves developed variable numbers of necrotic spots surrounded by mild mottling (Fig. 3b, lanes $\beta_{ND}NW_{Ec-3'}$). BSMV RNA and CP were difficult to detect, and these amounts were much lower than in Bd21-inoculated leaves or in NW-infected Bd3-1 leaves (Fig. 3b). Based on the consistency of these symptoms and observations elaborated on below, we believe that the $\beta_{ND}NW_{Ec-3'}$ phenotype results from chimeric TGB1 modifier effects that modulate Bd3-1 resistance to permit limited tissue invasion, while permitting *Bsr1*-associated necrosis and reduced virus accumulation.

$_{NW}$TGB1 residue K^{392} is a major *Bsr1* resistance-breaking determinant and residue K^{390} has a synergistic role

Comparisons of the *Pst*I–*Eco*RI fragment sequences from the ND18 and NW strains revealed differences at TGB1 positions 390, 392 and 404, consisting of lysine (K), arginine (R), threonine (T), glycine (G) and glutamic acid (E)

residues (Table 1). Site-specific mutagenesis was used to produce single mutants ($\beta_{ND}TGB1_{R390K}$, $\beta_{ND}TGB1_{T392K}$ and $\beta_{ND}TGB1_{G404E}$) containing $_{NW}$TGB1 variant codons, and complementary mutants ($\beta_{NW}TGB1_{K390R}$, $\beta_{NW}TGB1_{K392T}$ and $\beta_{NW}TGB1_{E404G}$) with $_{ND}$TGB1 residues (Fig. 4; see Supplementary Methods and Table S2 for construction of site-specific mutants). Double mutants ($\beta_{ND}TGB1_{R390K,T392K}$ and $\beta_{NW}TGB1_{K390R,K392T}$) with substitutions in both positions were also constructed.

All of the site-specific mutants developed systemic infections on barley and Bd21 (data not shown), but the Bd3-1 phenotype varied (Fig. 4). The $_{ND}$RNAβ_{G404E} and $_{NW}$RNAβ_{E404G} mutations had the same Bd3-1 phenotype as those of the parental $_{ND}$RNAβ and $_{NW}$RNAβ combinations (Fig. 4, lanes 2, 3, 7, 8 and 12). However, lysine substitutions to generate the $\beta_{ND}TGB1_{R390K}$ and $\beta_{ND}TGB1_{T392K}$ single mutants and the $\beta_{ND}TGB1_{R390K,T392K}$ double mutant each elicited visible Bd3-1 symptoms, but the disease phenotypes had distinct differences (Fig. 4, lanes 4–6). The $\beta_{ND}TGB1_{T392K}$ and $\beta_{ND}TGB1_{R390K,T392K}$ mutants elicited visible mosaic symptoms on Bd3-1, and the infected plants accumulated substantial amounts of BSMV (Fig. 4, lanes 5 and 6). In contrast, emerging leaves of $\beta_{ND}TGB1_{R390K}$-inoculated plants developed a barely discernible mottling with very low CP accumulation, accompanied by variable numbers of dispersed necrotic spots (Fig. 4, lane 4). These data suggest that the K^{392} residue in $_{NW}$TGB1 is involved in virulence on Bd3-1 and that both K residues in the $\beta_{ND}TGB1_{R390K,T392K}$ double mutant act synergistically to increase virus accumulation. Our interpretation of these results is that the $_{ND}$TGB1$_{R390K}$ mutant is able to mediate limited systemic movement in Bd3-1, and that the mutant protein elicits a *Bsr1*-associated HR in the invaded tissue.

The complementary $_{NW}$TGB1 mutants ($\beta_{NW}TGB1_{K390R}$, $\beta_{NW}TGB1_{K392T}$ and $\beta_{NW}TGB1_{K390R,K392T}$) RNAs (Fig. 4, Table 1) were co-inoculated with $_{ND}$RNAα and $_{ND}$RNAγ. The single substitution $\beta_{NW}TGB1_{K390R}$ and $\beta_{NW}TGB1_{K392T}$ mutant RNA combinations produced visible systemic infections on Bd3-1 accompanied by high levels of virus accumulation (Fig. 4, lanes 9 and 10). Only Bd3-1 plants inoculated with the $\beta_{NW}TGB1_{K390R,K392T}$ double mutant combination RNAs failed to develop a distinctive mosaic, but the emerging leaves instead exhibited very faint mottling symptoms coupled with a characteristic necrosis that appeared to originate from the parallel veins and spread along the veins (Fig. 4, lane 11). To explore the phenotypic effects of the $_{NW}$TGB1$_{K390R,K392T}$ mutant in greater detail, the time course of Bd3-1 infections was followed over a 2 week period (Fig. 5). In these infections, necrosis emanating from the vascular tissue continued to spread during leaf emergence and, by 14 days p.i., the leaves often died. Taken together, the $_{ND}$TGB1 and $_{NW}$TGB1 mutant effects provide evidence that background elements in the TGB1 proteins can affect BSMV movement and *Bsr1* resistance sufficiently to elicit variable Bd3-1 phenotypes.
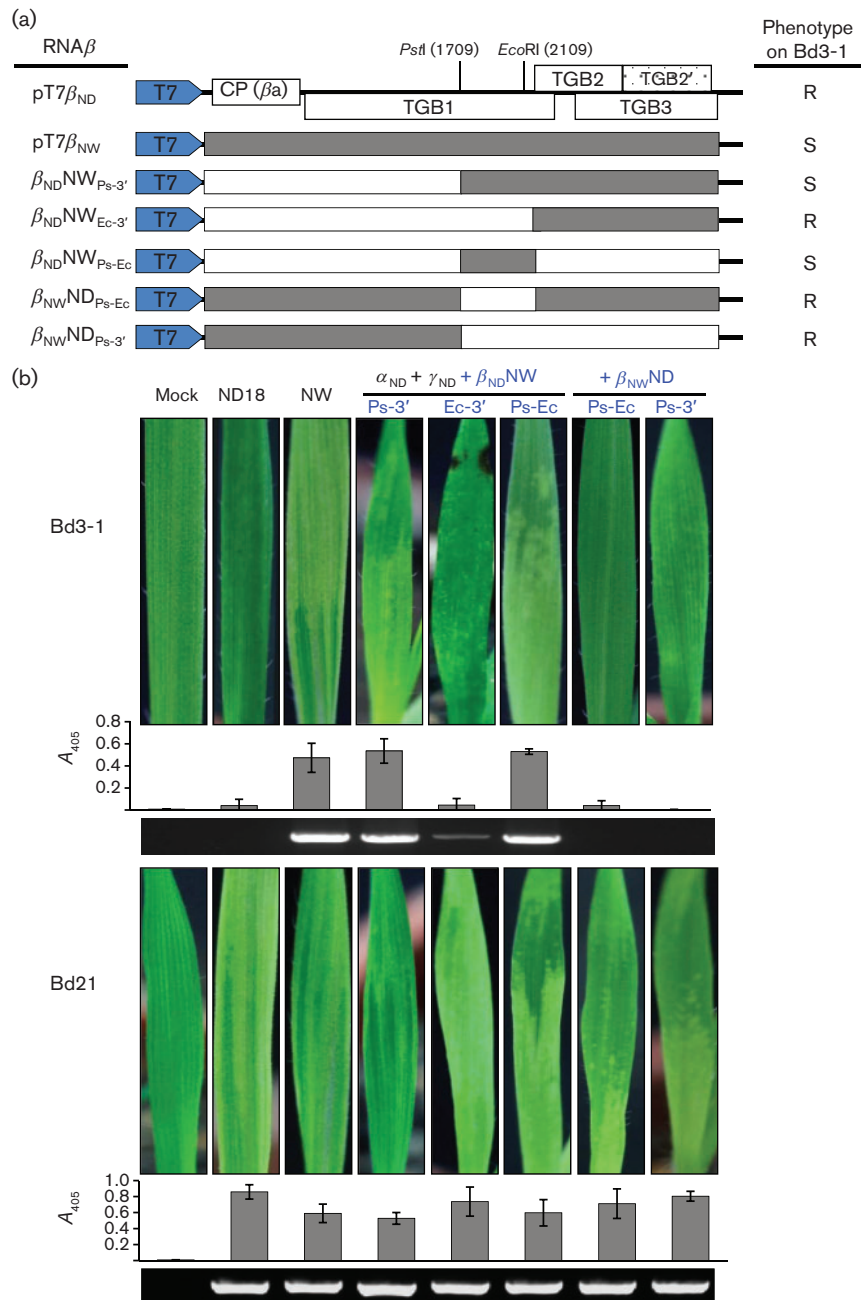
Fig. 3. Mapping of infection determinants of RNAβ chimeras on *B. distachyon* line Bd3-1. (a) Schematic representation of $_{ND}$RNAβ (pT7β_{ND}) and $_{NW}$RNAβ (pT7β_{NW}) cDNA clones and chimeric RNAβ recombinant clones. RNAβ plasmid designations are shown on the left, illustrations of the RNAβ plasmid chimeras are in the centre, and the Bd3-1 phenotype elicited by the different derivatives is indicated on the right. The blue pentagon in the schematic drawing represents the T7 promoter sequence used for *in vitro* transcription of the BSMV gRNAs, the β_{ND} sequence is illustrated by open white rectangles and the β_{NW} sequence is depicted by grey rectangles. The approximate locations of *Pst*I and *Eco*RI restriction sites used for chimeric RNAβ engineering are shown on the plasmid diagrams and the β_{ND} (white) and β_{NW} (grey) regions from which the sequence blocks originated are illustrated in the chimeras. (b) Symptoms and ELISA and RT-PCR detection of the infection phenotypes elicited after inoculation of pT7α_{ND} and pT7γ_{ND} wtRNA transcripts and RNAβ chimeras to Bd3-1 (top) and Bd21 (bottom). By 14 days p.i., all of the recombinant derivatives developed systemic infections with visible mosaic symptoms on Bd21, and the ELISA and RT-PCR bands below the leaves confirmed that the chimeras were infectious. On Bd3-1, the β_{ND}NW$_{Ps-3'}$ and β_{ND}NW$_{Ps-Ec}$ recombinant inoculations resulted in visible mosaic symptoms similar to NW strain infections on Bd3-1, whereas β_{ND}NW$_{Ec-3'}$-inoculated Bd3-1 plants developed a mild mottling phenotype on emerging leaves accompanied by very low intensities of the ELISA and RT-PCR bands. In addition to the mottling appearance on β_{ND}NW$_{Ec-3'}$, Bd3-1-inoculated leaves photographed at 5 days p.i., necrotic spots were often interspersed randomly along the leaf blade. In contrast, the β_{NW}ND$_{Ps-3'}$ and β_{NW}ND$_{Ps-Ec}$ chimeras failed to infect Bd3-1.

Table 1. Comparison of nucleotide and amino acid sequence and substitutions in the TGB1 helicase regions of the ND18 and NW strains

BSMV strain	Amino acid at TGB1 position					Bd3-1 phenotype*
	388	**389**	**390**	**392**	**404**	
ND18	GGT (Gly, G)	GGA (Gly, G)	AGG (Arg, R)	ACA (Thr, T)	GGA (Gly, G)	R
NW	GGT (Gly, G)	GGA (Gly, G)	AAG (Lys, K)	AAA (Lys, K)	GAA (Glu, E)	S
β_{ND}TGB1$_{R390K}$†	GGT (Gly, G)	GGA (Gly, G)	AAG (Lys, K)	ACA (Thr, T)	GGA (Gly, G)	R→S
β_{ND}TGB1$_{T392K}$†	GGT (Gly, G)	GGA (Gly, G)	AGG (Arg, R)	AAA (Lys, K)	GGA (Gly, G)	R→S
β_{ND}TGB1$_{R390K,T392K}$†	GGT (Gly, G)	GGA (Gly, G)	AAG (Lys, K)	AAA (Lys, K)	GGA (Gly, G)	R→S
β_{ND}TGB1$_{G404E}$†	GGT (Gly, G)	GGA (Gly, G)	AGG (Arg, R)	ACA (Thr, T)	GAA (Glu, E)	R
β_{ND}TGB1$_{T392A}$†	GGT (Gly, G)	GGA (Gly, G)	AGG (Arg, R)	GCA (Ala, A)	GGA (Gly, G)	R→S
β_{ND}TGB1$_{T392S}$†	GGT (Gly, G)	GGA (Gly, G)	AGG (Arg, R)	TCA (Ser, S)	GGA (Gly, G)	R→S
β_{ND}TGB1$_{R390A,T392A}$†	GGT (Gly, G)	GGA (Gly, G)	GCG (Ala, A)	GCA (Ala, A)	GGA (Gly, G)	R→S
β_{ND}TGB1$_{R390S,T392S}$†	GGT (Gly, G)	GGA (Gly, G)	AGC (Ser, S)	TCA (Ser, S)	GGA (Gly, G)	R→S
β_{ND}TGB1$_{G388A,G389A}$†	GCT (Ala, A)	GCA (Ala, A)	AGG (Arg, R)	ACA (Thr, T)	GGA (Gly, G)	R
β_{NW}TGB1$_{K390R}$‡	GGT (Gly, G)	GGA (Gly, G)	AGG (Arg, R)	AAA (Lys, K)	GAA (Glu, E)	S
β_{NW}TGB1$_{K392T}$‡	GGT (Gly, G)	GGA (Gly, G)	AAG (Lys, K)	ACA (Thr, T)	GAA (Glu, E)	S
β_{NW}TGB1$_{K390R, K392T}$‡	GGT (Gly, G)	GGA (Gly, G)	AGG (Arg, R)	ACA (Thr, T)	GAA (Glu, E)	S→R
β_{NW}TGB1$_{E404G}$‡	GGT (Gly, G)	GGA (Gly, G)	AAG (Lys, K)	AAA (Lys, K)	GGA (Gly, G)	S

*R, Resistant Bd3-1 reaction; S, susceptible Bd3-1 reaction; →, change in Bd3-1 phenotype.
†Site-specific changes in the $_{ND}$TGB1 protein.
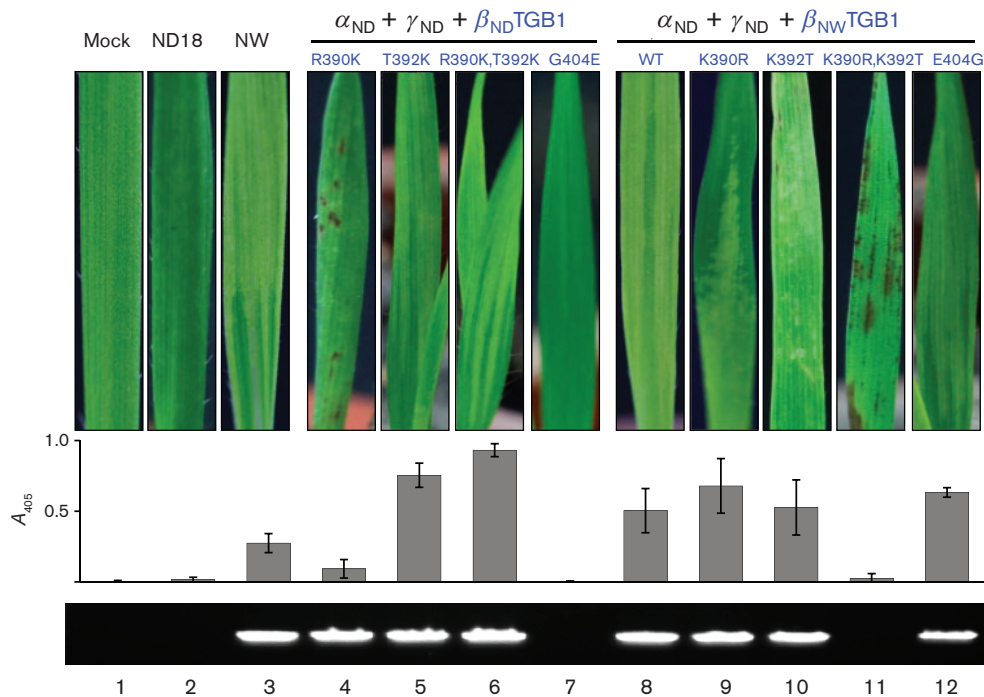‡Site-specific changes in the $_{NW}$TGB1 protein.

Fig. 4. Identification of key amino acid substitutions affecting the disease phenotype of *B. distachyon* Bd3-1 inoculated with $_{ND}$RNAβ and $_{NW}$RNAβ TGB1 mutants. Bd3-1 plants were co-inoculated with ND18 wtRNA α and γ transcripts and $_{ND}$RNAβ or $_{NW}$RNAβ mutants modified by incorporating site-specific amino acid mutations into TGB1 positions 390, 392 and 404, respectively. Leaves of plants photographed at 14 days p.i. (top), along with the results of ELISA CP detection (middle) and RNAγ RT-PCR amplification (bottom) from leaf extracts.
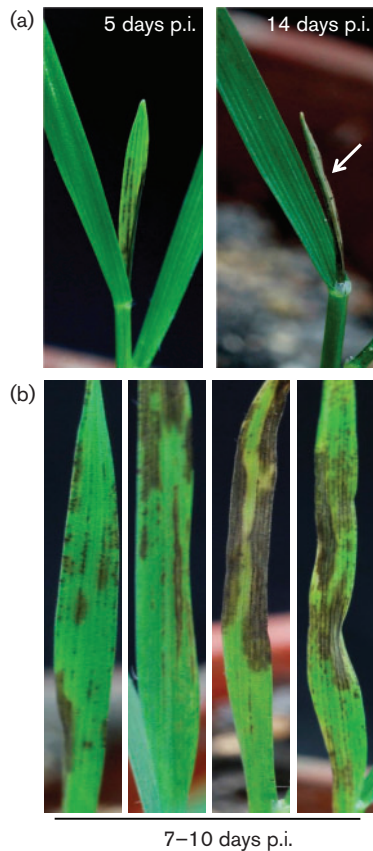
Fig. 5. Lethal phenotype elicited at different times after co-inoculation of Bd3-1 with ND18 α and γ wtRNAs plus $\beta_{NW}TGB1_{K390R,K392T}$. The phenotype on Bd3-1 plants was photographed at 5–14 days p.i. to document the spreading necrosis and lethal effects on emerging leaves. The necrosis usually resulted in death of the apical emerging leaves by 14 days p.i. and the leaves with intermediate necrotic stripes accumulated only trace amounts of CP and RNA (data not shown). (a) Phenotype on emerging leaves of a plant inoculated with the $\beta_{NW}TGB1_{K390R,K392T}$ mutant RNA to illustrate the progression of necrosis at 5 and 14 days p.i. The arrow shown at 14 days p.i. indicates a dead leaf that began developing necrosis at 4 days p.i. (b) Emerging leaves of plants inoculated with $\beta_{NW}TGB1_{K390R,K392T}$ mutant RNA. Photographs were taken between 7 and 10 days p.i.

Alanine and serine substitutions of $_{ND}TGB1$ residues R^{390} and T^{392} affect Bd3-1 infection phenotype

Sequence comparisons of $_{ND}TGB1$ revealed a putative internal *N*-myristoylation-like site (data not shown) encompassing the residue $G^{388}GRDTV^{393}$ that might potentially function during infection if post-translational TGB1 cleavages generated fragments with N-terminal glycine (G) residues (Gordon *et al.*, 1991; Traverso *et al.*, 2008). Because the G^{388} and G^{389} residues are critical components of the putative internal *N*-myristoylation site, we introduced site-specific alanine (A) or serine (S) substitutions to create the $\beta_{ND}TGB1_{G388A,G389A}$, $\beta_{ND}TGB1_{R390A,T392A}$, $\beta_{ND}TGB1_{R390S,T392S}$,

$\beta_{ND}TGB1_{T392A}$, and $\beta_{ND}TGB1_{T392S}$ mutants (see supplementary Methods). The results obtained after co-inoculation of Bd3-1 and Bd21 with the $_{ND}RNA$ mutants, and $_{ND}RNAs \alpha$ and γ revealed that the $_{ND}TGB1_{G388A,G389A}$ mutation did not alter the ND18 phenotype on either *B. distachyon* line (Fig. 6). These results suggest that myristoylation following possible post-translational cleavage of TGB1 does not have a substantial role in eliciting Bd3-1 resistance. However, the $\beta_{ND}TGB1_{R390A,T392A}$, $\beta_{ND}TGB1_{R390S,T392S}$, $\beta_{ND}TGB1_{T392A}$ and $\beta_{ND}TGB1_{T392S}$ substitution mutants exhibited fully susceptible phenotypes on both Bd3-1 and Bd21 (Fig. 6). The latter results reiterate our previous suggestion that both the R^{390} and T^{392} residues in $_{ND}TGB1$ are essential for elicitation of *Bsr1* resistance to ND18.

TGB1 background effects have roles in Bd3-1 phenotypic variation

To evaluate the virulence of additional BSMV strains, Bd3-1 and Bd21 seedlings were inoculated with leaf sap from barley plants inoculated with the BSMV ND18, NW, BJ, XJ, TY and CV21 strains (Fig. 7a, b). At 14 days p.i., all of the Bd21 plants inoculated with these strains were fully susceptible (Fig. 7b). However, the XJ-, TY- and CV21-inoculated Bd3-1 plants exhibited resistance similar to that of ND18, in which no visible phenotype appeared (Fig. 7a). Moreover, inspection of the XJ, TY and CV21 TGB1 sequences revealed that these strains contain R and T residues in positions corresponding to those of the ND18 R^{390} and T^{392} residues (Fig. 7c). Thus, these results indicate that the XJ, TY and CV21 strains elicit Bd3-1 *Bsr1* resistance gene functions similar to those elicited by ND18.

The BJ strain developed an entirely different phenotype from those of XJ, TY and CV21 that consisted of necrotic stripes on emerging leaves that appeared within 5 days p.i. The necrosis quickly spread along the veins and progressed to wilting and death of the plants by 14 days p.i. Sequence comparisons of BJ and the site-specific mutants were of special interest because the BJ strain has the same TGB1 genotype ($TGB1_{K390,T392}$) as the $_{NW}TGB1_{K392T}$ mutant, which elicits a fully virulent phenotype on Bd3-1 without signs of necrosis. Moreover, the $\beta_{ND}TGB1_{R390K}$ mutant, which develops a modulated systemic response consisting of necrotic spots, and the BJ strain ($_{BJ}TGB1_{K390,T392}$) have the same TGB1 amino acids at this position (Fig. 7c). In addition, all of the strains and mutants that elicited necrosis contained a $TGB1_{T392}$ residue, but varied in their K^{390} or R^{390} profiles. This observation again points to the importance of T392 in eliciting *Bsr1* resistance in Bd3-1.

DISCUSSION

This study extends our previous findings showing that the *B. distachyon* inbred line Bd3-1 harbours a gene (*Bsr1*) conditioning resistance to BSMV ND18 (Cui *et al.*, 2012).
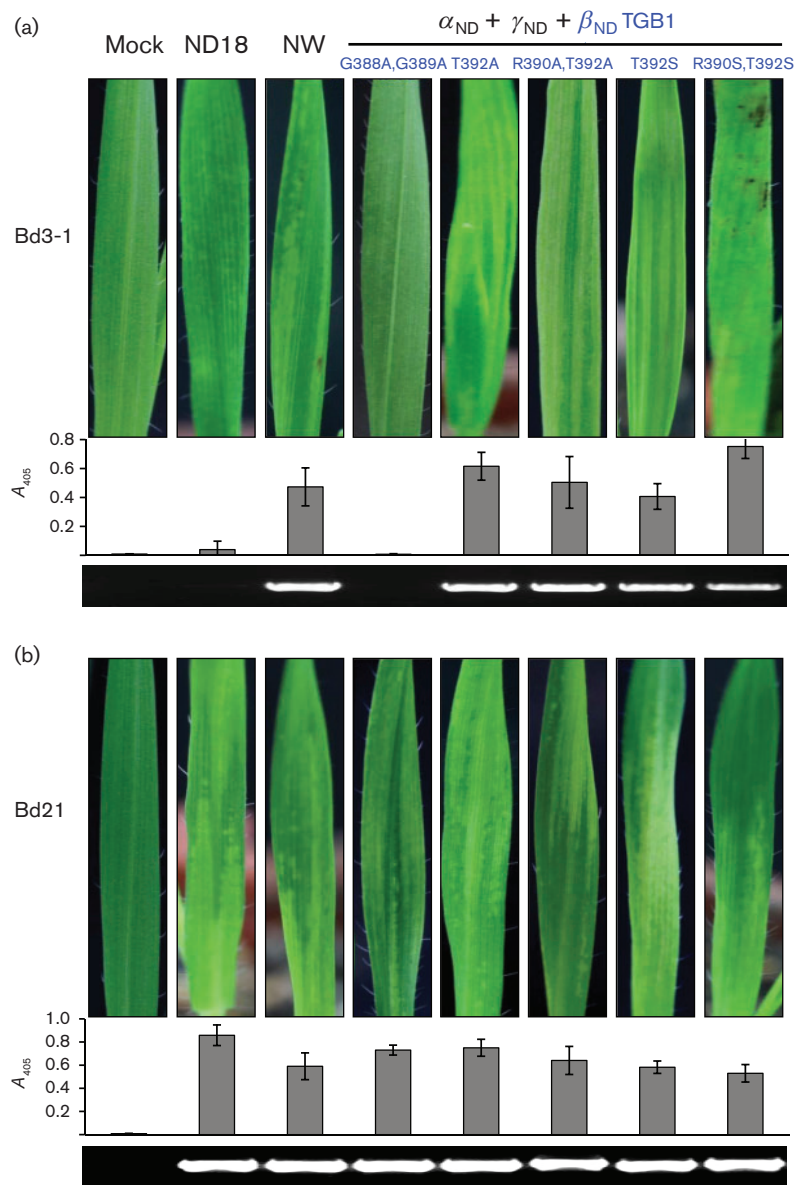
Fig. 6. Infection phenotypes elicited on Bd3-1 and Bd21 by site-specific alanine and serine substitutions in $_{ND}$TGB1 residues 388, 389, 390 and 392. Mutations were incorporated by site-specific mutagenesis, and $_{ND}$RNAs α and γ plus mutant $_{ND}$RNAβ transcripts were co-inoculated into Bd3-1 (a) and Bd21 (b) seedlings. Photographs of plants were taken at 14 days p.i. and leaves were harvested for ELISA and RT-PCR detection.

Our results show that, in contrast to ND18, the NW strain circumvents Bd3-1 resistance and is virulent on Bd3-1 (Cui *et al.*, 2012; Yuan *et al.*, 2011). We have mapped the resistance determinant to RNAβ, and have shown that the NW and ND18 α and γ gRNAs have only minor contributions to Bd3-1 resistance. More detailed mapping reveals that the major sequence conditioning Bd3-1 resistance resides within a unique *Pst*I–*Eco*RI fragment of $_{ND}$RNAβ. The 136 aa sequence within this fragment is located in the C-terminal half of the 58 kDa TGB1 protein, and consists of only three amino acid variations at positions 390, 392 and 404. Site-specific amino acid substitutions of ND18 and NW at position 404 failed to affect the respective phenotypes, but single exchanges of the $_{NW}$TGB1 390 or 392 residues into $_{ND}$TGB1 ($_{ND}$TGB1$_{R390K}$) or ($_{ND}$TGB1$_{T392K}$) or a double mutant ($_{ND}$TGB1$_{R390K,T392K}$) resulted in the ability to infect Bd3-1. However, incorporation of single

$_{ND}$TGB1 residues into the $_{NW}$TGB1 protein ($_{NW}$TGB1$_{K390R}$ and $_{NW}$TGB1$_{K392T}$) produced virus derivatives that were able to infect Bd3-1. These results imply that the K^{390} and K^{392} residues in $_{NW}$TGB1 can compensate for each other to circumvent Bd3-1 resistance. In addition, alanine and serine substitutions of either of the R^{390} or T^{392} residues into $_{ND}$TGB1 enables the mutants to infect Bd3-1. Moreover, comparisons of XJ, TY and CV21 TGB1 sequences are in agreement with the conclusion that TGB1 positions 390 and 392 are critical residues affecting Bd3-1 *Bsr1* resistance, and that analysis of such residues in uncharacterized BSMV strains may provide a potential tool to predict *Bsr1* resistance interactions.

What might be the nature of such interactions? Our current studies show that amino acids involved in avirulent ND18 and virulent NW infections of Bd3-1 are located
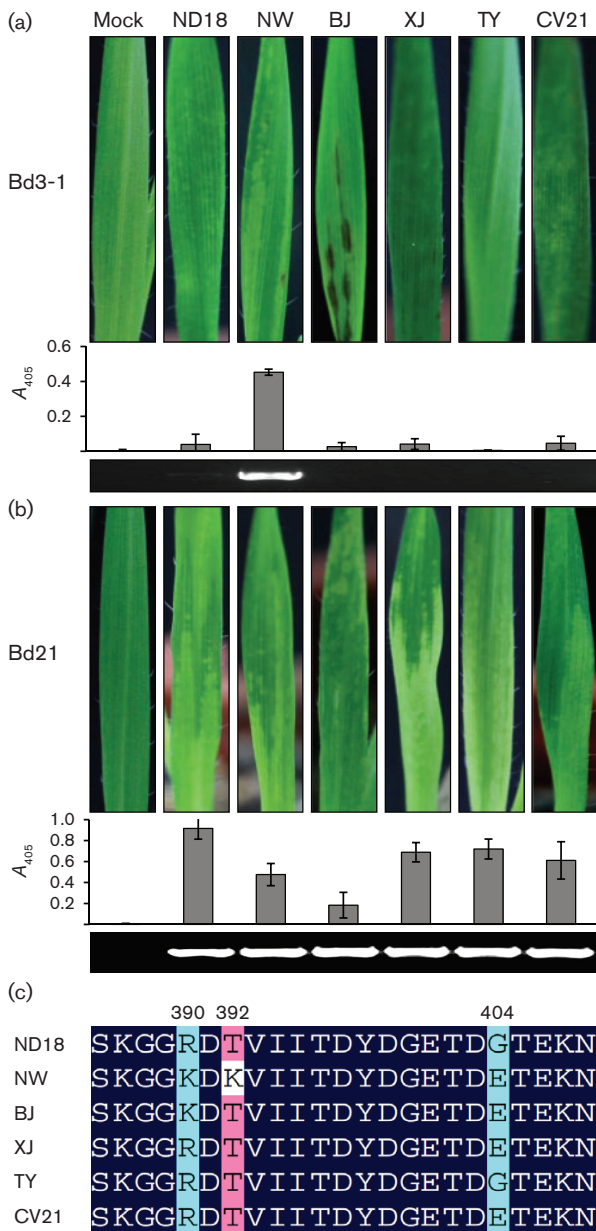
Fig. 7. Differential virulence of BSMV isolates on *B. distachyon* line Bd3-1. (a) Bd3-1 seedlings inoculated with leaf sap from barley infected with the ND18, NW, BJ, XJ, TY and CV21 strains of BSMV (top). Note: photographs were taken of inoculated plants at 14 days p.i., except for Bd3-1 plants inoculated with the BJ isolate, which were photographed at 6 days p.i. In contrast to the NW virulent control, BJ-inoculated Bd3-1 leaves showed the first signs of necrosis at ~4 days p.i., the necrosis spread rapidly after the plants began to wilt, and by 14 days p.i. the inoculated plants had died and dried out completely. ND18, XJ, TY and CV21-inoculated Bd3-1 plants normally failed to develop signs of infection or accumulate CP (middle) or BSMV RNA (bottom) on Bd3-1. (b) Systemic infection response and CP and RNA accumulation in Bd21 plants inoculated with the BSMV strains. (c) Comparisons of the amino acid sequences surrounding the TGB1 virulence motif of different BSMV isolates. Numbers represent the amino acid positions of the ND18 and NW TGB1 proteins.

within the helicase domain of the TGB1 protein. Previous studies indicate that TGB1 is a multifunctional protein that participates in a number of movement-related events. Moreover, the helicase domain, which contains seven motifs that are conserved in several virus genera (Morozov & Solovyev, 2003; Verchot-Lubicz *et al.*, 2010), has several biochemical functions, all of which are required for cell-to-cell movement (Jackson *et al.*, 2009). Amongst these functions are protein–protein interactions (Leshchiner *et al.*, 2006; Lim *et al.*, 2008), RNA binding (Donald *et al.*, 1997; Leshchiner *et al.*, 2006; Lim *et al.*, 2008) and RNA helicase (Kalinina *et al.*, 2002) activities. We have previously shown that $_{ND}$TGB1 homologous binding is compromised by site-specific amino acid substitutions in helicase motifs I (residue 259) and II (residues 339 and 340), and that disrupting these interactions interferes with cell-to-cell movement of ND18 (Lim *et al.*, 2009). However, the TGB1$_{390}$ and TGB1$_{392}$ mutations do not compromise critical TGB1 movement functions, but do affect the Bd3-1 disease phenotype. Hence, the TGB1$_{390}$ and TGB1$_{392}$ amino acids appear to specifically affect Bd3-1 *Bsr1* R gene activities.

A plausible mechanism for Bd3-1 resistance to ND18 is that the $_{ND}$TGB1 and Bd3-1 *Bsr1* proteins engage in interactions that activate the *Bsr1* resistance pathway, and that lysine, serine and alanine substitutions incorporated at $_{ND}$TGB1 residues 390 and 392 disrupt these interactions. The results also suggest that the ability of the NW strain to circumvent Bd3-1 resistance is a consequence of the absence of $_{NW}$TGB1–*Bsr1* interactions. Such a mechanism is consistent with the quadratic check model classically found in plant pathogen 'gene-for-gene' interactions (Flor, 1971). In the case of BSMV–*B. distachyon* interactions, we posit that, in addition to its other activities, the $_{ND}$TGB1 protein is an elicitor that functions by interacting physically with the Bd3-1 *Bsr1* protein to culminate in a resistance response. Moreover, we hypothesize that $_{ND}$TGB1 does not interact with the non-functional Bd21 *Bsr1* allelic protein, and hence ND18 is virulent on Bd21. Conversely, the $_{NW}$TGB1 protein is unable to interact with either of the Bd3-1 or Bd21 *Bsr1* allelic proteins, and hence the NW strain is virulent on both hosts.

Our data also provide indirect evidence supporting the hypothesis that Bd3-1 resistance involves an HR typical of responses often associated with dominant R genes (Gururani *et al.*, 2012). This evidence is based on the unveiling of a necrotic response by site-specific substitutions in $_{ND}$TGB1 and $_{NW}$TGB1 mutants. The clearest example that an HR may be involved in resistance is the spreading necrosis occurring after Bd3-1 inoculation with the β_{NW}TGB1$_{K390R,K392T}$ mutant, and to a lesser extent the necrotic spots exhibited in Bd3-1 leaves inoculated with the β_{ND}TGB1$_{R390K}$ mutant. Variable necrosis associated with disease phenotypes of these mutants and lower abundances of BSMV RNA and CP in emerging leaves indicates that these phenotypes are elicited by TGB1 interactions, but that the mutants compromise the Bd3-1 resistance response sufficiently to permit limited

vascular movement of BSMV to emerging secondary leaves while maintaining *Bsr1* HR activities. The necrosis associated with these two mutants ($\beta_{NW}TGB1_{K390R,K392T}$ and $\beta_{ND}TGB1_{R390K}$), coupled with the rapid wilting and death of Bd3-1 plants inoculated with the BJ strain (genotype= $_{BJ}TGB1_{K390,T392}$) RNAs, and the low levels of CP and viral RNA accumulation in these infections lends additional credence for an HR elicited by *Bsr1*. Our premise is that the *Bsr1* protein functions in part via eliciting an HR in infected tissue that is typical of classical R genes functioning in plant disease interactions (Gassmann & Bhattacharjee, 2012; Heath, 2000). Under this scenario, the Bd3-1 Bsr1 protein interacts with the $_{ND}TGB1$ protein, but not with the $_{NW}TGB1$ protein, to elicit a resistance signalling cascade that constrains ND18 infections to the initially infected cell foci.

We have recently cloned both candidate *Bsr1* alleles, and our preliminary results indicate that the $_{ND}TGB1$ protein is able to bind directly to the Bd3-1 Bsr1 protein, but not to the Bd21 Bsr1 allelic protein (L. Yan & D. Li, unpublished data). However, as predicted in the model above, $_{NW}TGB1$ is unable to bind to either of the R proteins. Moreover, we have also accumulated biological evidence demonstrating that gene-specific TGB1–*Bsr1* allelic combinations result in specific HR activities that reflect the BSMV–*B. distachyon* disease phenotypes. These results, which we plan to describe in a forthcoming manuscript, combined with the data presented above, provide a convincing scenario whereby Bd3-1 resistance involves an HR whose elicitation requires $_{ND}TGB1$–Bd3-1 *Bsr1* binding activities.

METHODS

Construction of full-length infectious Type (TY) and North Dakota 18 (ND18) BSMV cDNA clones and the origins of the strains have been described previously (Petty *et al.*, 1988, 1989). The Norwich (NW) strain (provided by Dr R. Hull, John Innes Centre, Norwich, UK) was originally recovered as an isolate from the Rothamsted strain, and its physico-chemical and biological properties were first described by Lane (1974). Seed transmission of the CV21 strain was studied in North Dakota by R. G. Timian (Timian, 1974), and this strain was apparently called the 'moderate strain LQ' (Dr M. C. Edwards, personal communication) in descriptions of the biological properties of BSMV strains collected before 1965 (McKinney & Greeley, 1965). The two Chinese strains, Beijing (BJ) (Sun *et al.*, 2007) and Xinjiang (XJ) (Xie *et al.*, 1981), along with the CV21 strain, were kindly provided by Professors Xianchao Sun (College of Plant Protection, South-west University, China) and Bingsheng Qiu (Institute of Microbiology, Chinese Academy of Sciences).

Growth of barley (Black Hulless and Yangmai 2-9114) and *B. distachyon* (lines Bd3-1, Bd21 and Bd21-3) plants was conducted as described previously (Cui *et al.*, 2012; Lim *et al.*, 2009; Yuan *et al.*, 2011). A more detailed accounting of optimal conditions for *B. distachyon* growth and maintenance, BSMV inoculation conditions, analyses of BSMV CP and RNA abundance, and inoculation and assessment of disease phenotype during infection is given in the supplementary Methods. Explicit details of methods used for construction of BSMV NW strain infectious cDNA clones, RNAβ chimeras and site-specific mutant plasmids, and sequencing of various plasmids are also presented in the supplementary Methods.

ACKNOWLEDGEMENTS

REFERENCES

Brkljacic, J., Grotewold, E., Scholl, R., Mockler, T., Garvin, D. F., Vain, P., Brutnell, T., Sibout, R., Bevan, M. & other authors (2011). *Brachypodium* as a model for the grasses: today and the future. *Plant Physiol* **157**, 3–13.

Cui, Y., Lee, M. Y., Huo, N., Bragg, J., Yan, L., Yuan, C., Li, C., Holditch, S. J., Xie, J. & other authors (2012). Fine mapping of the *Bsr1* barley stripe mosaic virus resistance gene in the model grass *Brachypodium distachyon*. *PLoS ONE* **7**, e38333.

Donald, R. G. & Jackson, A. O. (1994). The barley stripe mosaic virus γ b gene encodes a multifunctional cysteine-rich protein that affects pathogenesis. *Plant Cell* **6**, 1593–1606.

Donald, R. G., Lawrence, D. M. & Jackson, A. O. (1997). The barley stripe mosaic virus 58-kilodalton β(b) protein is a multifunctional RNA binding protein. *J Virol* **71**, 1538–1546.

Edwards, M. C., Bragg, J. & Jackson, A. O. (2006). Natural resistance mechanisms to viruses in barley. In *Natural Resistance Mechanisms of Plants to Viruses*, pp. 465–501. Edited by G. Loebenstein & J. P. Carr. Dordrecht: Springer.

Flor, H. H. (1971). Current status of the gene-for-gene concept. *Annu Rev Phytopathol* **9**, 275–296.

Garvin, D. F., Gu, Y.-Q., Hasterok, R., Hazen, S. P., Jenkins, G., Mockler, T. C., Mur, L. A. J. & Vogel, J. P. (2008). Development of genetic and genomic research resources for *Brachypodium distachyon*, a new model system for grass crop research. *Crop Sci* **48**, S69–S84.

Gassmann, W. & Bhattacharjee, S. (2012). Effector-triggered immunity signaling: from gene-for-gene pathways to protein–protein interaction networks. *Mol Plant Microbe Interact* **25**, 862–868.

Gordon, J. I., Duronio, R. J., Rudnick, D. A., Adams, S. P. & Gokel, G. W. (1991). Protein *N*-myristoylation. *J Biol Chem* **266**, 8647–8650.

Gururani, M. A., Venkatesh, J., Upadhyaya, C. P., Nookaraju, A., Pandey, S. K. & Park, S. W. (2012). Plant disease resistance genes: current status and future directions. *Physiol Mol Plant Pathol* **78**, 51–65.

Heath, M. C. (2000). Hypersensitive response-related death. *Plant Mol Biol* **44**, 321–334.

Jackson, A. O. & Lane, L. C. (1981). Hordeiviruses. In *Handbook of Plant Virus Infections and Comparative Diagnosis*, pp. 565–625. Edited by E. Kwistakk. Amsterdam: Elsevier.

Jackson, A. O., Petty, I. T. D., Jones, R. W., Edwards, M. C. & French, R. (1991a). Analysis of barley stripe mosaic virus pathogenicity. *Semin Virol* **2**, 107–119.

Jackson, A. O., Petty, I. T. D., Jones, R. W., Edwards, M. C. & French, R. (1991b). Molecular genetic analysis of barley stripe mosaic virus pathogenicity determinants. *Can J Plant Pathol* **13**, 163–177.

Jackson, A. O., Lim, H.-S., Bragg, J., Ganesan, U. & Lee, M. Y. (2009). Hordeivirus replication, movement, and pathogenesis. *Annu Rev Phytopathol* **47**, 385–422.

Kalinina, N. O., Rakitina, D. V., Solovyev, A. G., Schiemann, J. & Morozov, S. Y. (2002). RNA helicase activity of the plant virus movement proteins encoded by the first gene of the triple gene block. *Virology* **296**, 321–329.

Kang, B.-C., Yeam, I. & Jahn, M. M. (2005). Genetics of plant virus resistance. *Annu Rev Phytopathol* **43**, 581–621.

Lane, L. C. (1974). The components of barley stripe mosaic and related viruses. *Virology* **58**, 323–333.

Leshchiner, A. D., Solovyev, A. G., Morozov, S. Y. & Kalinina, N. O. (2006). A minimal region in the NTPase/helicase domain of the TGBp1 plant virus movement protein is responsible for ATPase activity and cooperative RNA binding. *J Gen Virol* **87**, 3087–3095.

Lim, H.-S., Bragg, J. N., Ganesan, U., Lawrence, D. M., Yu, J., Isogai, M., Hammond, J. & Jackson, A. O. (2008). Triple gene block protein interactions involved in movement of barley stripe mosaic virus. *J Virol* **82**, 4991–5006.

Lim, H.-S., Bragg, J. N., Ganesan, U., Ruzin, S., Schichnes, D., Lee, M. Y., Vaira, A. M., Ryu, K. H., Hammond, J. & Jackson, A. O. (2009). Subcellular localization of the barley stripe mosaic virus triple gene block proteins. *J Virol* **83**, 9432–9448.

Maule, A. J., Caranta, C. & Boulton, M. I. (2007). Sources of natural resistance to plant viruses: status and prospects. *Mol Plant Pathol* **8**, 223–231.

McKinney, H. H. & Greeley, L. W. (1965). Biological characteristics of barley stripe mosaic virus strains and their evolution. *US Department of Agriculture Technical Bulletin* no. 1324.

Moffett, P. (2009). Mechanisms of recognition in dominant R gene mediated resistance. *Adv Virus Res* **75**, 1–33.

Morozov, S. Y. & Solovyev, A. G. (2003). Triple gene block: modular design of a multifunctional machine for plant virus movement. *J Gen Virol* **84**, 1351–1366.

Opanowicz, M., Vain, P., Draper, J., Parker, D. & Doonan, J. H. (2008). *Brachypodium distachyon*: making hay with a wild grass. *Trends Plant Sci* **13**, 172–177.

Petty, I. T. D., Hunter, B. G. & Jackson, A. O. (1988). A novel strategy for one-step cloning of full-length cDNA and its application to the genome of barley stripe mosaic virus. *Gene* **74**, 423–432.

Petty, I. T. D., Hunter, B. G., Wei, N. & Jackson, A. O. (1989). Infectious barley stripe mosaic virus RNA transcribed *in vitro* from full-length genomic cDNA clones. *Virology* **171**, 342–349.

Petty, I. T. D., Donald, R. G. K. & Jackson, A. O. (1994). Multiple genetic determinants of barley stripe mosaic virus influence lesion phenotype on *Chenopodium amaranticolor*. *Virology* **198**, 218–226.

Renner, T., Bragg, J., Driscoll, H. E., Cho, J., Jackson, A. O. & Specht, C. D. (2009). Virus-induced gene silencing in the culinary ginger (*Zingiber officinale*): an effective mechanism for down-regulating gene expression in tropical monocots. *Mol Plant* **2**, 1084–1094.

Santoso, A. & Edwards, M. C. (2003). Identification of the nucleotide substitutions required for barley stripe mosaic hordeivirus pathogenicity to barley possessing the *rsm1* gene. *Phytopathology* **93**, S75–S76.

Sun, X., An, D., Qing, L. & Yang, S. (2007). Identification of the barley stripe mosaic virus (BSMV) from Beijing. *J Southwest Univ (Nat Sci Ed)* **29**, 51–54.

Timian, R. G. (1974). The range of symbiosis of barley and *Barley stripe mosaic virus*. *Phytopathology* **64**, 342–345.

Traverso, J. A., Meinnel, T. & Giglione, C. (2008). Expanded impact of protein *N*-myristoylation in plants. *Plant Signal Behav* **3**, 501–502.

van Ooijen, G., Mayr, G., Kasiem, M. M., Albrecht, M., Cornelissen, B. J. & Takken, F. L. (2008). Structure–function analysis of the NB-ARC domain of plant disease resistance proteins. *J Exp Bot* **59**, 1383–1397.

Verchot-Lubicz, J., Torrance, L., Solovyev, A. G., Morozov, S. Y., Jackson, A. O. & Gilmer, D. (2010). Varied movement strategies employed by triple gene block-encoding viruses. *Mol Plant Microbe Interact* **23**, 1231–1247.

Vogel, J. & Bragg, J. (2009). *Brachypodium distachyon*, a new model for the Triticeae. In *Genetics and Genomics of the Triticeae*, pp. 427–449. Edited by G. J. Muehlbauer & C. Feuillet. New York: Springer.

Vogel, J. P., Garvin, D. F., Mockler, T. C., Schmutz, J., Rokhsar, D., Bevan, M. W., Barry, K., Lucas, S., Harmon-Smith, M. & other authors (2010). Genome sequencing and analysis of the model grass *Brachypodium distachyon*. *Nature* **463**, 763–768.

Weiland, J. J. & Edwards, M. C. (1996). A single nucleotide substitution in the α a gene confers oat pathogenicity to barley stripe mosaic virus strain ND18. *Mol Plant Microbe Interact* **9**, 62–67.

Whitham, S., Dinesh-Kumar, S. P., Choi, D., Hehl, R., Corr, C. & Baker, B. (1994). The product of the tobacco mosaic virus resistance gene *N*: similarity to Toll and the interleukin-1 receptor. *Cell* **78**, 1101–1115.

Xie, H., Wang, Z., Li, W. & Ni, S. (1981). Occurence of barley stripe mosaic virus in Xinjiang. *Acta Phytopathologica Sinica* **11**, 11–14.

Yuan, C., Li, C., Yan, L., Jackson, A. O., Liu, Z., Han, C., Yu, J. & Li, D. (2011). A high throughput barley stripe mosaic virus vector for virus induced gene silencing in monocots and dicots. *PLoS ONE* **6**, e26468.